

Supporting Information
Architecture-Controlled Synthesis of M_xO_y ($M=Ni$, Fe , Cu)
Microfibres from Seaweed Biomass for High-Performance Lithium
Ion Battery Anodes

Chunxiao Lv, Xianfeng Yang, Ahmad Umar, Yanzhi Xia, Yi(Alec) Jia, Lu
Shang, Tierui Zhang and Dongjiang Yang

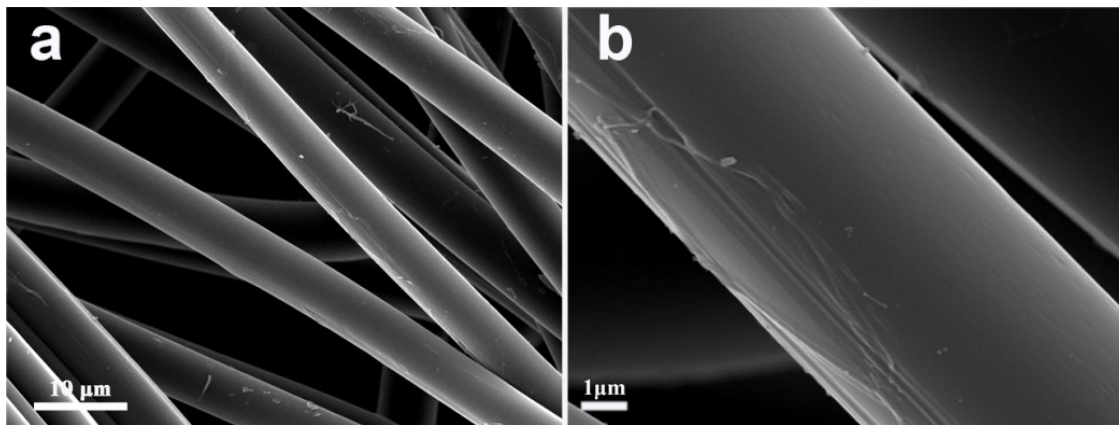


Fig. S1. (a,b) SEM images of Ca-AF.

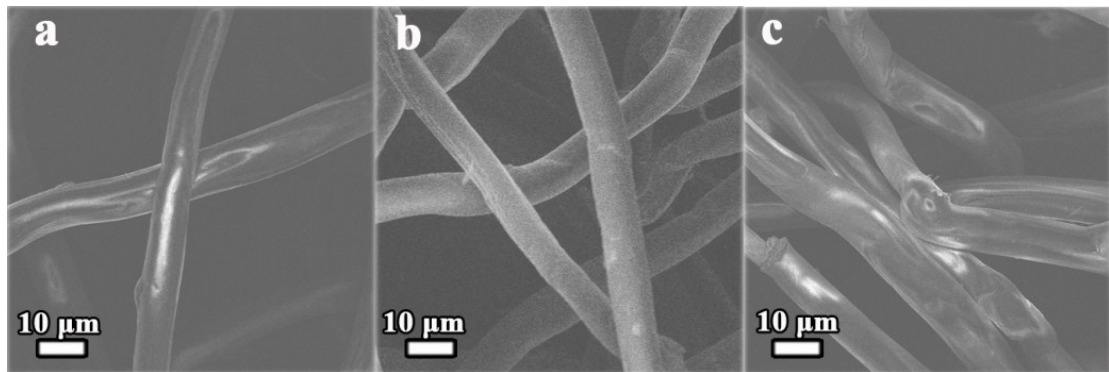


Fig. S2. (a,b,c) SEM images of M-AF ($M=$ Ni, Fe, Cu).

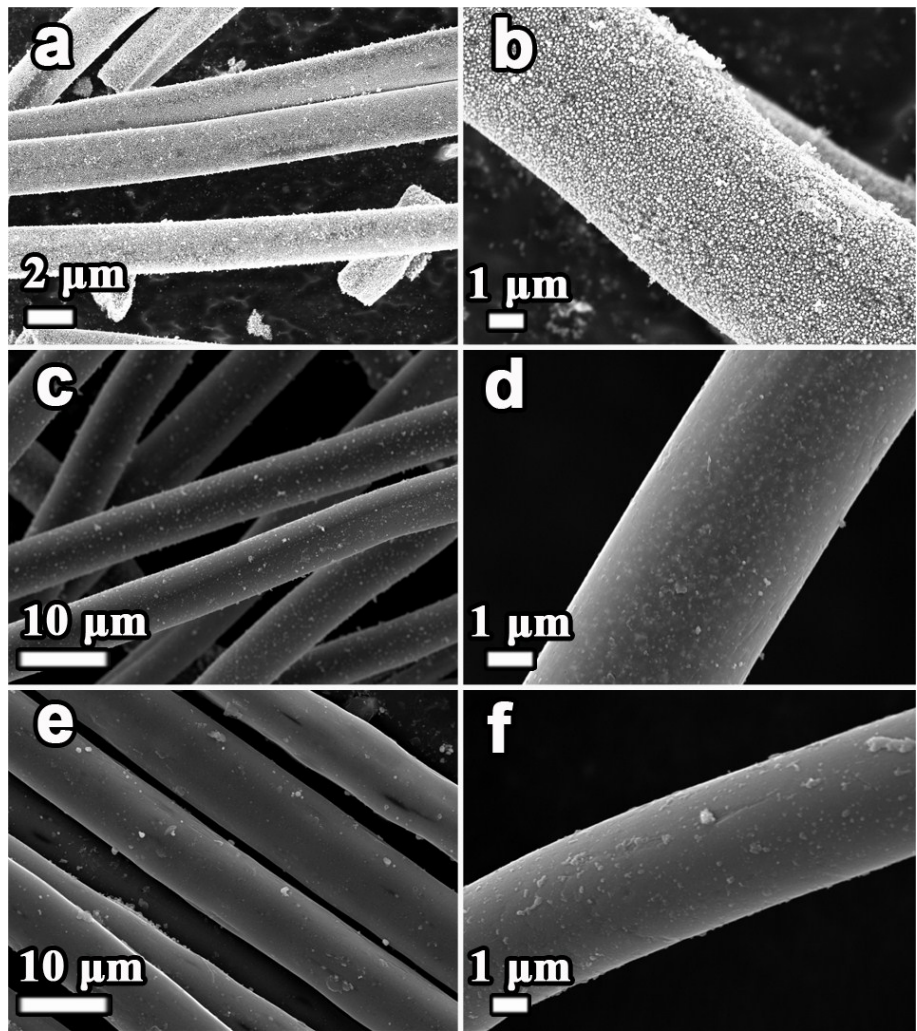


Fig. S3. SEM images of (a,b) Ni-CF, (c,d) Fe-CF and (e,f) Cu-CF.

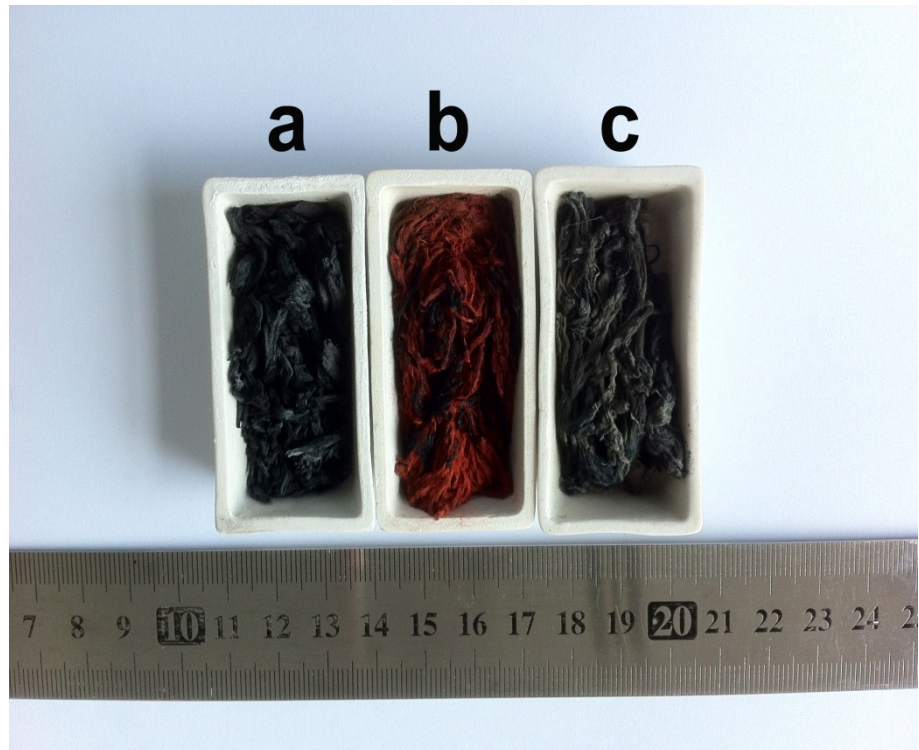


Fig. S4. Photographic image of (a) NiO/Ni/C-F,(b) C@Fe₂O₃-F and (c) CuO-HF.

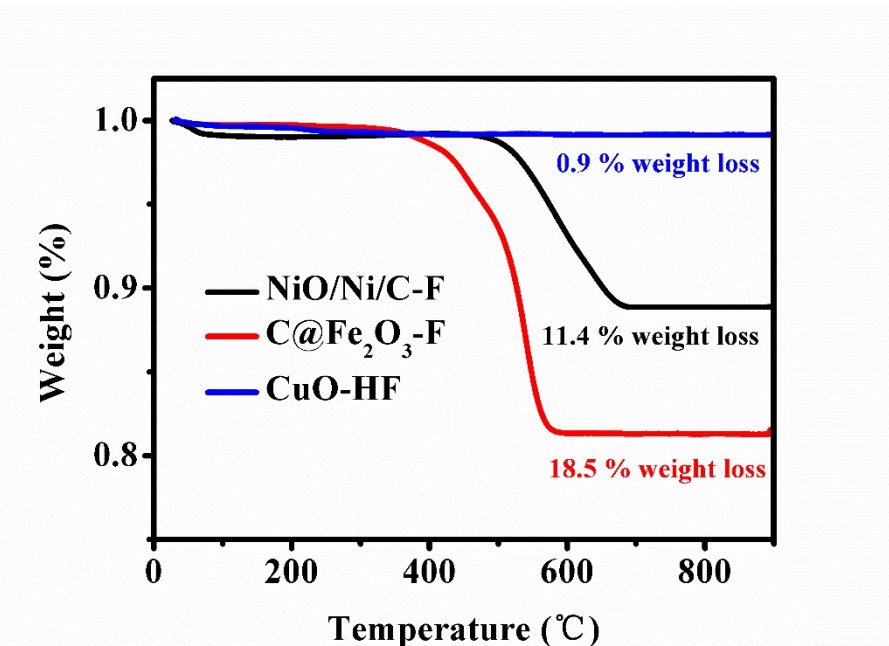


Fig. S5. TGA Characterizations of NiO/Ni/C-F, C@Fe₂O₃-F and CuO-HF.

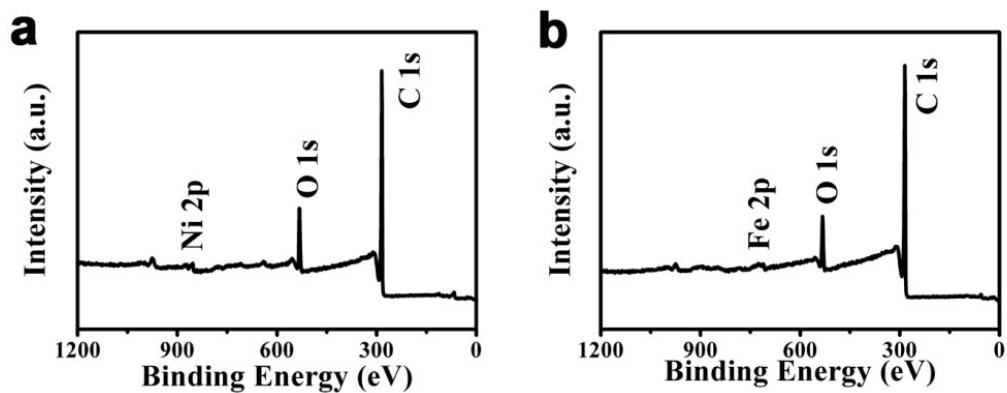


Fig. S6. Full survey scan spectrum XPS spectras of (a) NiO/Ni/C-F and (b) C@Fe₂O₃-F.

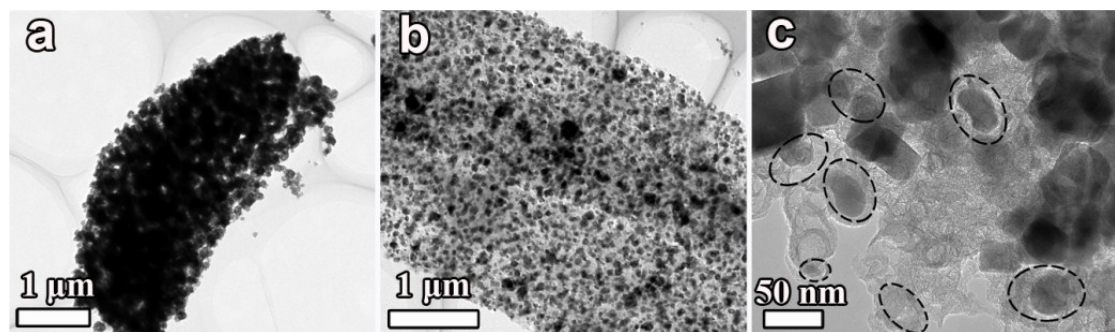


Fig. S7. TEM images of (a) NiO/Ni/C-F and (b,c) C@Fe₂O₃-F.

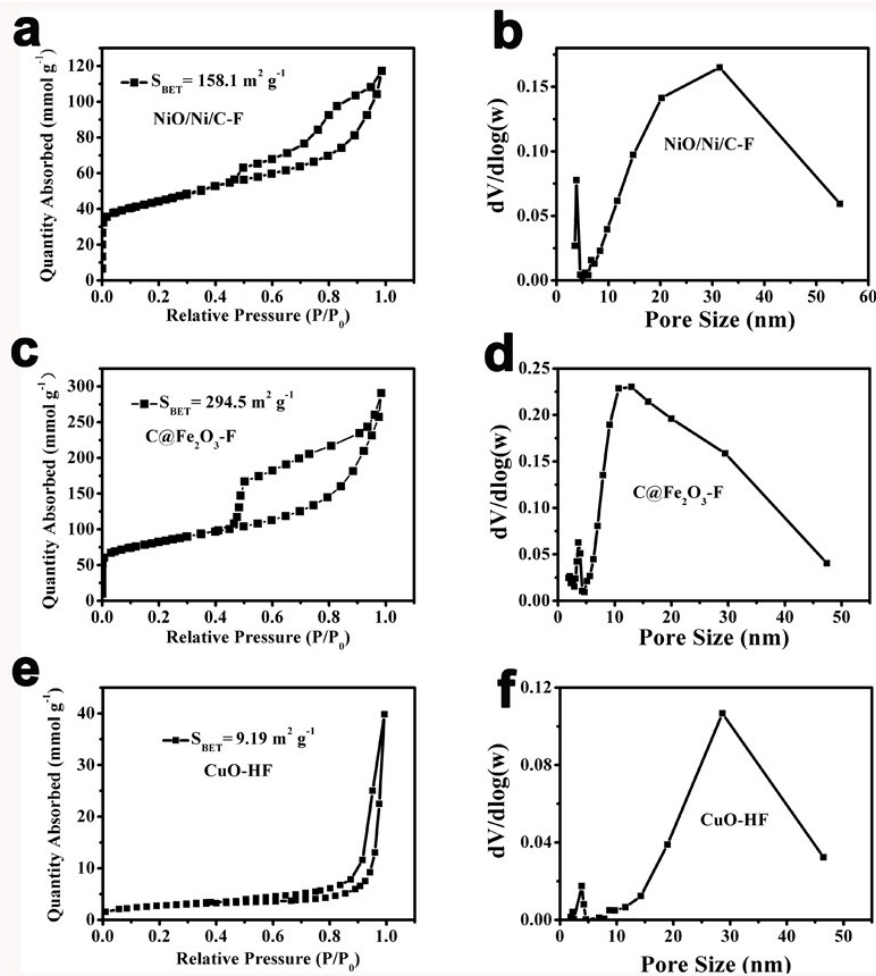


Fig. S8. (a,c,d)Nitrogen adsorption-desorption isotherm and (b,d,e) the corresponding pore size distribution curve of NiO/Ni/C-F, C@Fe₂O₃-F and CuO-HF.

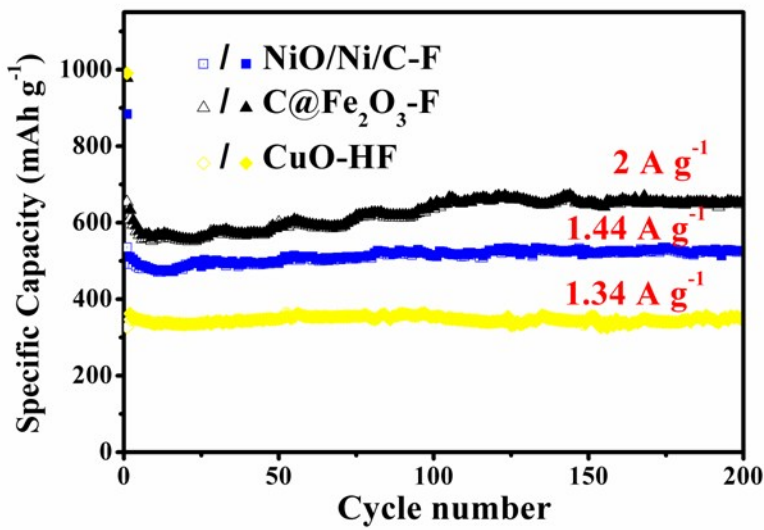


Fig. S9. Cycling performance of NiO/Ni/C-F, C@Fe₂O₃-F and CuO-HF electrodes at current density of 2 A g⁻¹, 1.44 A g⁻¹ and 1.34 A g⁻¹, respectively.

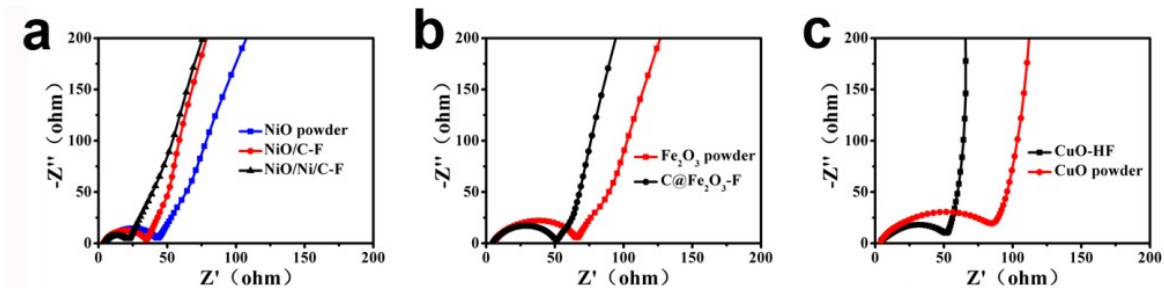


Fig. S10. Electrochemical impedance spectroscopy (EIS) for NiO/Ni/C-F, C@Fe₂O₃-F, CuO-HF electrodes and the comparative samples.

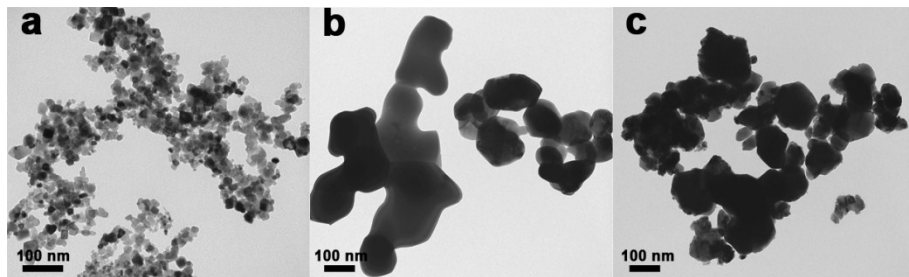


Fig. S11. TEM of commercial (a) NiO powder, (b) Fe₂O₃ powder and (c) CuO powder.